

Evaluation of S/N Diagram in Welded Joints Based on Different Fatigue Failure Criteria

Saeed Jouzdani¹

Department of Mechanical Engineering,
Khomeinishahr Branch, Islamic Azad University, Khomeinishahr/Isfahan,
Iran
E-mail: saeed.jouzdani@iaukhsh.ac.ir

Ali Heidari^{2, *}

Department of Mechanical Engineering,
Khomeinishahr Branch, Islamic Azad University, Khomeinishahr/Isfahan,
Iran
E-mail: heidari@iaukhsh.ac.ir

*Corresponding author

Received: 13 December 2019, Revised: 16 May 2020, Accepted: 18 May 2020

Abstract: One of the most important problems in the welded Joints is the low fatigue strength due to the residual stresses. Purpose of this study is to investigate the effect of residual stresses on S/N diagram of the welded joints. For this purpose, welding process of two plates is firstly modeled on a precise and three-dimensional model. This simulation has been carried out in two non-coupled thermal-mechanical steps, including the birth and death of elements technique, presence of molten flow inside melting pool and latent heat generated by phase transformations in the simulator program. Thermal and mechanical results of the program are compared with numerical and experimental results of other researchers, which indicates acceptable accuracy of the program. In the next step, effect of welding process residual stress on S/N diagram is investigated with two different fatigue criteria, which the results indicate a decrease in the fatigue strength. Goodman's modified fatigue criterion shows 88%, and Gerber's criterion shows 78% of reduction. Finally, by examining effect of changes in air flow parameters and preheating, the results showed that the transient air flow reduced fatigue strength for 5% and preheating, results in a 9% increase in fatigue strength.

Keywords: Fatigue Criteria, Residual Stress, S/N Diagram, Welding Process

Reference: Saeed Jouzdani, Ali Heidari, "Evaluation of S/N Diagram in Welded Joints Based on Different Fatigue Failure Criteria", Int J of Advanced Design and Manufacturing Technology, Vol. 13/No. 3, 2020, pp. 67–74. DOI: 10.30495/admt.2020.1885273.1164.

Biographical notes: Saeed Jouzdani received his MSc in Mechanical Engineering from Khomeinishahr Branch of Islamic Azad University 2018. His research interests include the field of applied mechanical design. Ali Heidari received his PhD in Mechanical Engineering from Isfahan University of Technology 2014. He is currently Assistant Professor at the Department of Mechanical Engineering, Khomeinishahr Branch, Islamic Azad University, Khomeinishahr, Iran. More than 19 journal papers, 39 accepted conference papers and 1 published book are the results of his researches so far. He has been involved in teaching and research activities for more than 13 years. His current research interest includes Thermal stresses, Metal forming, Mechanical design and Optimization.

1 INTRODUCTION

Welding process is one of the most common methods of joining in metal structures; the reason for this is its ability to joint different geometric shapes to each other [1]. One of the main defects in the welded joints is the failure caused by the fatigue phenomenon [1-3]. Typically, fatigue strength of welded joints is much less than strength of the base metal [4]; due to factors such as residual stresses, areas with different mechanical properties and non-homogeneous geometry in welded joints. Among them, the residual stresses have a deep effect on the behavior of high cycle fatigue life [4-5]. The residual stresses distribution prediction in welded structures is very complicated by the presence of different physical phenomena such as heat, electricity or mechanical work [6-7]. Due to the difficulties of precise measurement of amount of residual stresses [8], therefore, numerical methods are often used to determine stress distribution. Today, fatigue behavior analysis of welding joints with multi-axial stresses have not been completely solved [9], therefore different methods have been proposed to obtain an equivalent single-axial stress [10-12].

An equivalent effective stress hypothesis was proposed by Sonsino for soft steel welding under a non-proportional multi-axial loading, which did not take into account the actual amount of residual stresses [13, 14]. A definitive method to predict fatigue life of the joints with spot welding process, taking into account the residual stresses was developed by Bae et al. [15]. In this method, maximum value of main stress at the edge of metal is defined as the midrange stress component in the Goodman relation.

Karsovsky et al. [16] investigated effect of post weld heat treatment on the residual stresses. They simulated the welding process with 5 passes and then, using critical plane method and Findley's injury criterion [17], found that possibility of failure was not related to the post weld heat treatment. Vassansarjah et al. [18] conducted a study of multi-pass processes using conventional TIG and A-TIG methods; it was found that A-TIG process had a lower residual tensile stress. Yuguan et al. [19] studied the stress concentration factors in K-shaped welded joints using finite element method. They also simulated the temperature field, and the distribution of residual stress using the Element birth and death technology. The results indicated that the residual stress was higher than yield strength and was improved after heat treatment.

Ganesh et al. [20] performed thermal-mechanical analysis of tungsten-arc welding process with protective gas on 316LN austenitic stainless steel. After a detailed study and numerical modeling, they validated results with two non-destructive methods of X-ray and ultrasonic waves testing. Vassansargaja et al. [21]

investigated welding process effect of type 316LN austenitic stainless steel on residual stresses. To this end, they developed three models with different geometries for the welding of tungsten arc with protective gas. After experimental work, numerical results were confirmed by performing radiographic test and micro structural analysis. Non-destructive ultrasonic wave test was used to measure residual stresses.

Bhatti et al. [22] investigated thermal-mechanical properties of materials in different steel types on residual stresses. They found that in order to evaluate residual stress in carbon steels, heat capacity for thermal analysis is an important parameter. Lopez-Jauregi et al. [23-24] described an alternative method to assess High Cycle Fatigue (HCF) life prediction based on numerically estimated RS values. Results have shown good correspondence for the HCF range, with a maximum average error of 15% in stress for the studied configurations.

Wang et al. [25] investigated effects of residual stresses on fatigue behavior of T-joint joints by fracture mechanics based on coupled stress and energy criterion. The finite element method was used to determine the residual stresses in welding process; it was determined that effects of residual stresses on yield strength for crack radii smaller than 0.5 mm were significant and for crack radii greater than or equal to 0.5 mm were insignificant. Also, effects of residual stresses can change direction of crack curvature and reduce ductility. In addition, predicted fatigue strength with this method has good compliance with proposed value in the IIW standard.

The aim of this study is to investigate effect of residual stresses in tungsten arc welding with CO₂ protective gas on S/N diagram of welding joints. For this purpose, welding process is first simulated with non-coupled method and then accuracy of its results is validated. Then, based on two different fatigue criteria, effect of residual stresses on the fatigue strength was investigated. Moreover, the effects of transient air flow and preheating temperature on residual stresses and S/N diagram have been investigated as two new works in this study too.

2 FINITE ELEMENT MODEL

In this study, welding process of two similar plates with a width of 80 mm, length of 200 mm and a thickness of 10 mm was studied. Figure 1 shows geometry of model on the X-Y plane and shows joining form of two plates. Type of process is tungsten arc welding with CO₂ protective gas. In order to achieve an accurate simulation, modeling is carried out in a three-dimensional method. With respect to the symmetry, only half of the model is simulated.

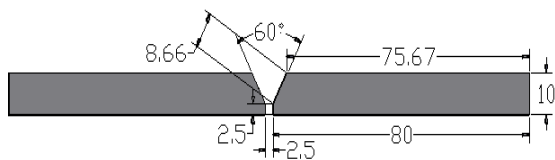


Fig. 1 Front view of model in X-Y plane.

Figure 2 shows model meshing method. Due to the severe gradient of temperature and stress around the weld zone, this zone is more important. Therefore, a finer meshing is used in this zone [26]. “Table 1” specifies the welding parameters. Figure 3 shows the order of passes.

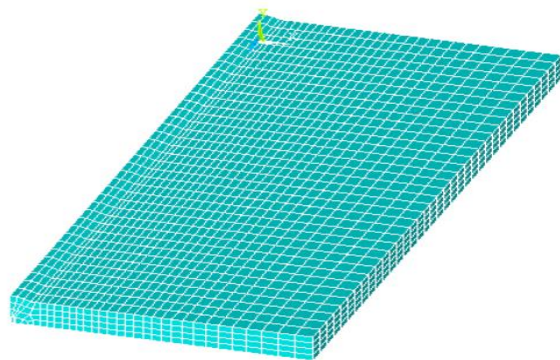


Fig. 2 Model meshing.

Table 1 Welding parameters for each pass [24]

| Pass | Current (A) | Voltage (V) | Welding speed (mm/s) |
|------|-------------|-------------|----------------------|
| 1 | 275 | 28.2 | 9.1 |
| 2 | 275 | 28.2 | 8.1 |
| 3 | 275 | 28.2 | 6.1 |

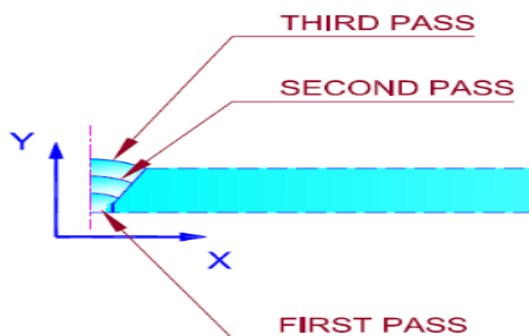


Fig. 3 Order of welding passes.

The time between the first and second passes is equal to 35 seconds, between the second and third passes is 37

seconds, and after the third pass solution continues until achieving ambient temperature. Welding efficiency is 75% for the first pass, 80% for the second pass and 90% for the third pass [24]. In order to simulate three weld passes, the birth and death of elements are used, in which, instead of eliminating the elements, the ability of death of elements is used, in such a way that for the death of the elements, the decreasing coefficient is multiplied by their hardness, and although the force vector of the dead element is zero, it shows itself in the force vector of the elements. On the other hand, mass, specific heat and other effects are close to zero and do not add to total mass and energy sum of the whole model, and for birth of the elements, the above coefficients return to their original value too [27].

3 MATERIAL PROPERTIES

In this study, the work piece is made of S275JR. Properties of this steel and weight percent of its constituent elements are given in “Table 2” [24].

Table 2 Chemical Compositions (%) of S275JR steel [24]

| C | Mn | Cu | S | P |
|-------|------|-------|--------|--------|
| <0.21 | <1.5 | <0.55 | <0.035 | <0.035 |

Thermo-physical and mechanical properties of the material in terms of temperature are shown in “Figs. 4 and 5”. Work-hardening rule is also considered as linear isotropic.

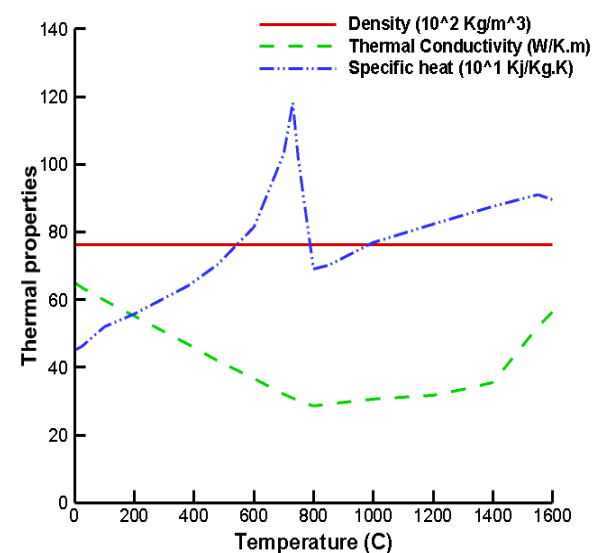


Fig. 4 Temperature-dependent thermal physics properties of S275JR steel [24].

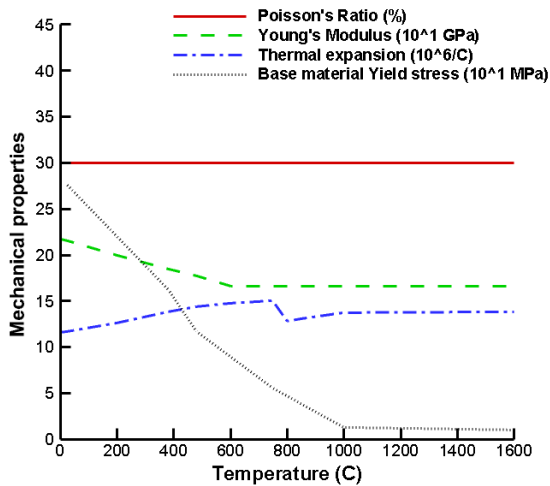


Fig. 5 Temperature-dependent mechanical properties of S275JR steel [24].

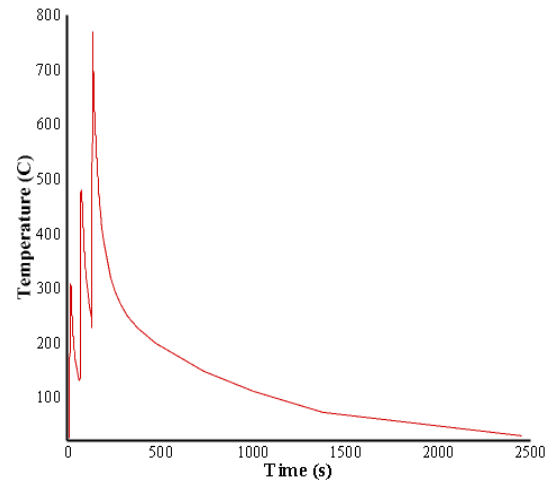


Fig. 6 Thermal history of indicator point.

4 THERMAL SOLUTION RESULTS

Since thermal stresses obtained from plastic strain, effect of stresses on phase transformations, and changes in heat transfer coefficient due to surface strains are insignificant, mechanical and thermal equations can be solved independently using non-coupled solution [5-8]. Due to symmetry, convective heat transfer coefficient in central line is zero and in the rest of surfaces it is equal to $15 \text{ W/m}^2\text{k}$. Ambient temperature is 25°C . In order to consider the effect of melting pool fluid flow, thermal conductivity coefficient is increased at a temperature above the melting point with a coefficient. Effect of latent heat of phase change is also considered by increasing specific heat coefficient at the phase change temperature [4], [6]. In the thermal model, the solid70 element that is a three-dimensional, eight-node element with thermal conductivity ability is used. This element has one degree of freedom (temperature) at each node and is suitable for three-dimensional transient thermal flows. In this study, Goldak's double-ellipsoidal heat source model has been used to simulate the thermal source. In "Fig. 6", thermal history of a point with position of $x = 8.08 \text{ mm}$, $y = 10 \text{ mm}$ and $z = 22.2 \text{ mm}$, that is called thermal solution indicator point, is shown up to 2437 seconds after start of welding. Obviously, an increase in temperature will be observed at each point corresponding to each welding pass. In "Fig. 7", thermal history of indicator point is compared with experimental and numerical results of other researchers. Temperature measurement is done by camera and thermocouple. This comparison shows that numerical results of the present study are in suitable accordance with experimental results.

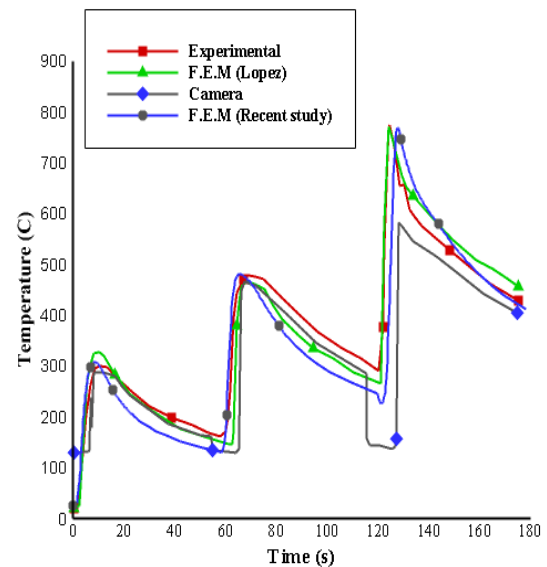


Fig. 7 Thermal history comparison with experimental and numerical results of other researchers.

5 MECHANICAL SOLUTION RESULTS

In first step of simulation, based on 3D thermal solution, temperature distribution model was determined during welding process. In next step, obtained temperature history is applied to mechanical model as a thermal load, and after mechanical solution, stress distribution will be achieved. Mechanical model is exactly the same as the thermal model (except the type of element and boundary conditions). Element used in mechanical model is the solid185 that is a three dimensional, eight-node, and structural element.

In “Fig. 8”, distribution of residual stresses on a line in x-z plane with initial point coordinates $x_1 = 23.75, z_1 = 0, y_1 = 10, \text{ mm}$ and end point $x_2 = 23.75, z_2 = 200, y_2 = 10, \text{ mm}$, which is called mechanical solution indicator line is provided. As it can be seen, stress values along welding length have different values that maximum tensile stress based on numerical solution of present study, is 136/23 MPa, at a distance of $z = 110 \text{ mm}$ from center of coordinate system. In this figure, the numerical results of mechanical solution are compared with experimental and numerical results of other researchers. This comparison shows that the results of this study follow the experimental residual stresses trend suitably.

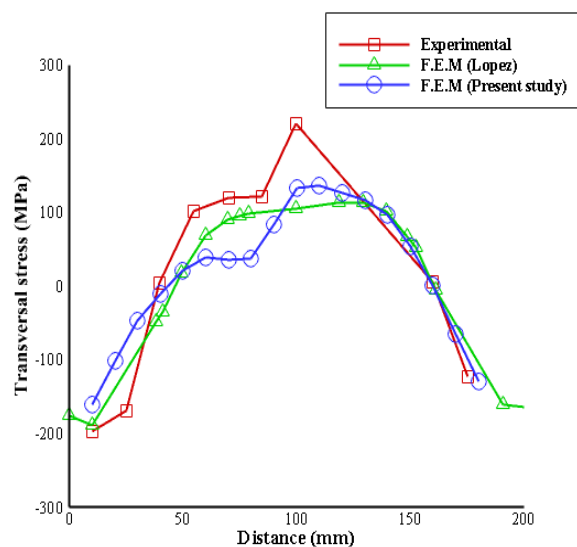


Fig. 8 Comparison of transversal residual stresses on the indicator line with experimental and numerical results of other researchers.

6 S/N DIAGRAM CONSIDERING RESIDUAL STRESSES OF WELDING PROCESS

First, this section describes how to apply residual stress on modified Goodman's fatigue criterion and to obtain a S/N diagram for which residual stress is included. Figure 9 shows S/N diagram of S275JR steel without applying residual stresses. Modified Goodman's criterion is as follows [23]:

$$\frac{\sigma_a}{S_f} + \frac{\sigma_m}{S_{ut}} = \frac{1}{n} \tag{1}$$

Which, σ_a is amplitude component of stress, σ_m is midrange component of stress, S_f is fatigue strength, S_{ut} is ultimate base metal tensile strength and n is safety factor.

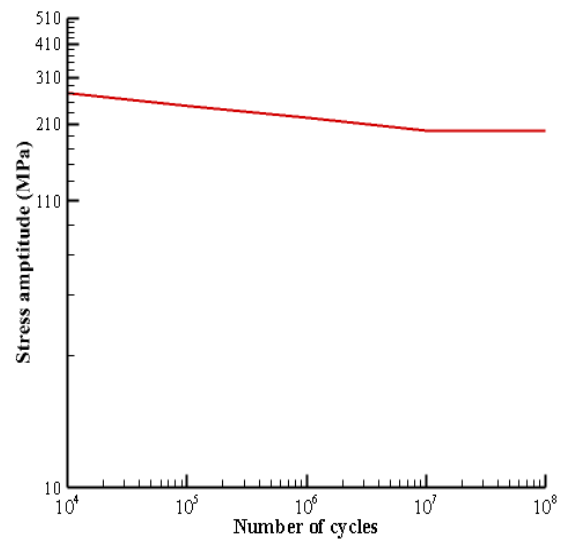


Fig. 9 S/N diagram of S275JR steel [23].

Modified Goodman's criterion considering residual stress and $n = 1$ is as follows [23]:

$$\frac{\sigma_{a-res}}{S_f} + \frac{\sigma_{res}}{S_{ut}} = 1 \tag{2}$$

Which, σ_{a-res} is amplitude component in the presence of residual stresses and σ_{res} is the maximum amount of residual stresses that is obtained from the simulation and considered as a midrange component of stress. To apply the residual stresses on S/N diagram and to calculate the fatigue strength by considering residual stresses, Equation 2 is rewritten as follows:

$$\sigma_{a-res} = S_f \left(1 - \frac{\sigma_{res}}{S_{ut}} \right) \tag{3}$$

Therefore, how to plot S/N diagram for welded joints will be such that, regarding the constant of the residual stress and ultimate tensile strength in different cycles of S/N diagram, different values of fatigue strength in each cycle based on the base metal S / N diagram are determined, and placed in equation (3). In this way, the amount of new amplitude component is obtained by the presence of residual stresses for the welded joints. By repeating this process in different cycles, the amount of new amplitude components in each cycle is calculated, and based on these values, S/N diagram will be plotted considering presence of residual stresses. Similarly, the S/N diagram can be obtained by considering residual stress using Gerber's criterion. The Gerber relation with respect to the residual stresses and $n = 1$ is as follows:

$$\sigma_{a-res} = S_f \left[1 - \left(\frac{\sigma_{res}}{S_{ut}} \right)^2 \right] \quad (4)$$

In “Fig. 10”, S/N diagram of welded component obtained from modified Goodman's Fatigue criterion and Gerber's fatigue criterion are compared to S/N diagram of the base material. As shown in “Fig. 10”, residual stresses have a significant effect on fatigue diagram of welded component and greatly reduce fatigue strength. This issue shows the need of solutions to reduce residual stresses of the welding process. On the other hand, it is observed that Gerber's criterion shows approximately 78 percent, and Goodman's criterion shows approximately 88 percent reduction in fatigue strength. In other words, modified Goodman's fatigue criterion is more prudent than Gerber's fatigue criterion.

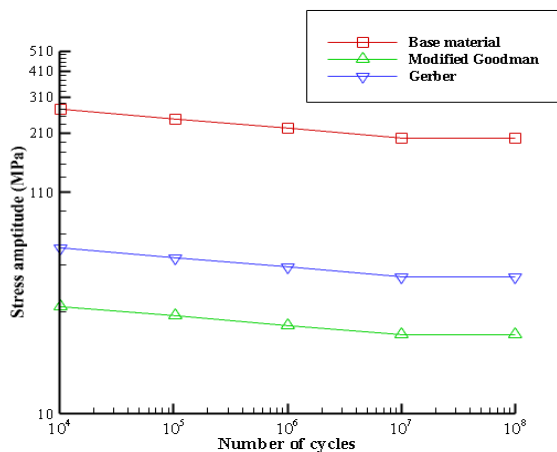


Fig. 10 Comparison S/N diagrams obtained from the modified Goodman's criteria, Gerber's criterion and base metal.

7 EFFECT OF TRANSIENT AIR FLOW AND PREHEATING TEMPERATURE

Blowing an air flow on the joints has increased coefficient of air convection heat transfer and accelerated cooling. In “Fig. 11”, S/N diagrams obtained from modified Goodman's criteria have been compared in two modes of blowing air flow on the joints and presence of static air. As shown in this figure, blowing an air flow on the piece ($h_A = 25W/m^2k$) resulted in a reduction of approximately 5% of fatigue strength of the piece relative to static air flow ($h_A = 15W/m^2k$).

In “Fig. 12”, S/N diagrams obtained from modified Goodman's criteria are compared in two modes of pre-heated and non-pre-heated. The results of this research show that preheating heat treatment on the joints reduces equivalent residual stress and results in approximately

9% increase in fatigue strength of the joints when not preheated. Preheat temperature is 100 °C .

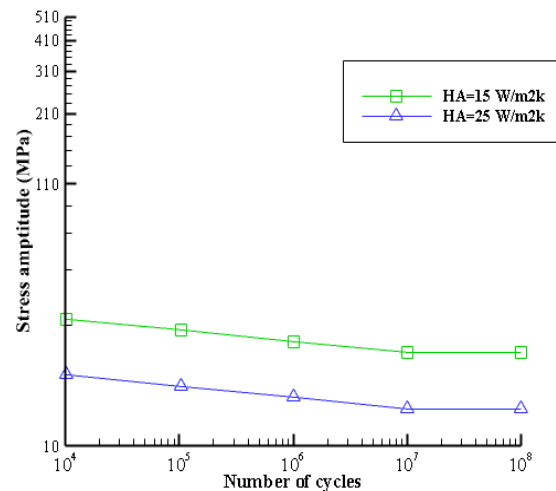


Fig. 11 Effect of convective heat transfer coefficient on S/N diagram.

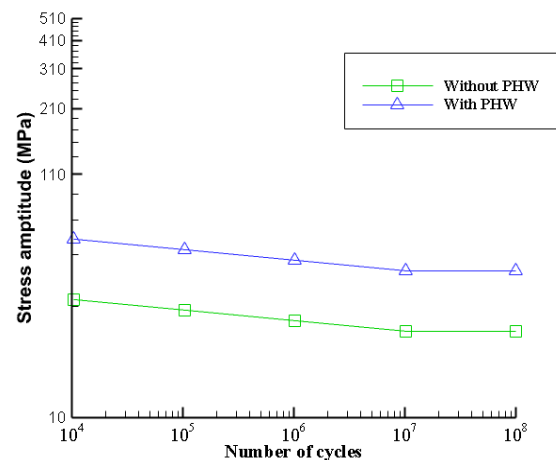


Fig. 12 Effect of preheating heat treatment on S/N diagram.

8 CONCLUSION

In the present study, process of arc welding with tungsten electrodes and CO2 protective gas is simulated in a three-dimensional and high precision and validated. Based on mechanical solution results, effects of residual stresses created in welded joints on S/N diagrams and fatigue strength have been evaluated. Key findings of this research are:

- The residual stresses have a significant effect on the fatigue diagram of welded joints and greatly reduce the fatigue strength, which this issue shows urgent need for solutions to reduce residual stresses.

- The Gerber's criterion and Goodman's criterion reduce fatigue strength by approximately 78 percent, and approximately 88 percent, respectively. In other words, the modified Goodman's fatigue criterion is more cautious than Gerber's fatigue criterion.

- Blowing airflow on the joints increases equivalent residual stresses and reduces approximately 5% of fatigue strength in S/N diagram relative to static airflow.

- Preheat heat treatment on the joints reduces equivalent residual stress and results in approximately 9% fatigue strength in the S / N diagram than when this treatment is not performed.

8 APPENDIX OR NOMENCLATURE

| | |
|------------------|--|
| σ_a | : Amplitude component of stress |
| σ_m | : Midrange component of stress |
| S_f | : Fatigue strength |
| S_{ut} | : Ultimate strength |
| σ_{a-res} | : Amplitude component in presence of residual stresses |
| σ_{res} | : Maximum amount of residual stresses |
| n | : Safety factor |
| h_A | : Convection heat transfer coefficient |
| PHW | : Welding process with preheating |

REFERENCES

- [1] Marin, T., Nicoletto, G., Fatigue Design of Welded Joints using the Finite Element Method and the 2007 Asme Div. 2 Master Curve, Fracture and Structural Integrity, Vol. 3, No. 9, 2009, pp. 76–84.
- [2] Carpinteri, A., Spagnoli, A., and Vantadori, S., Multiaxial Fatigue Life Estimation in Welded Joints Using the Critical Plane Approach, International Journal of Fatigue, Vol. 31, No. 1, 2009, pp. 188–196.
- [3] Livieri, P., Lazzarin, P., Fatigue Strength of Steel and Aluminum Welded Joints Based on Generalized Stress Intensity Factors and Local Strain Energy Values, International Journal of Fracture, Vol. 133, No. 3, 2005, pp. 247–276.
- [4] Maddox, S. J., Fatigue Strength of Welded Structures: Woodhead publishing, 1991.
- [5] Kong, F., Ma, J., and Kovacevic, R., Numerical and Experimental Study of Thermally Induced Residual Stress in the Hybrid Laser–GMA Welding Process, Journal of Materials Processing Technology, Vol. 211, No. 6, 2011, pp. 1102–1111.
- [6] Chang, P. H., Teng, T. L., Numerical and Experimental Investigations On the Residual Stresses of The Butt-Welded Joints, Computational Materials Science, Vol. 29, No. 4, 2004, pp. 511–522.
- [7] Messler, R. W., Principles of Welding: Processes, Physics, Chemistry, and Metallurgy: John Wiley & Sons, 2008.
- [8] Asadi, M., Goldak, J. A., Nielsen, J., Zhou, J., Tchernov, S., and Downey, D., Analysis of Predicted Residual Stress in a Weld and Comparison with Experimental Data Using Regression Model, Int J Mech Mater Des, No. 5, 2009, pp. 353–364.
- [9] Bruder, T., Störzel, K., Baumgartner, J., and Hanselka, H., Evaluation of Nominal and Local Stress Based Approaches for the Fatigue Assessment of Seam Welds, International Journal of Fatigue, Vol. 34, No. 1, 2012, pp. 86–102.
- [10] Bokesjö, M., Al-Emrani, M., and Svensson, T., Fatigue Strength of Fillet Welds Subjected to Multi-Axial Stresses, International Journal of Fatigue, Vol. 44, 2012, pp. 21–31.
- [11] BS7608, Code of Practice for Fatigue Design and Assessment of Steel Structures: British Standards Institution, 1993.
- [12] Hobbacher, A., Recommendations for Fatigue Design of Welded Joints and Components: OH: Welding Research Council Shaker Heights, 2009.
- [13] Sonsino, C. M., Overview of the State of the Art On Multiaxial Fatigue of Welds, European Structural Integrity Society, Vol. 25, 1999, pp. 195–217.
- [14] Sonsino, C. M., Multiaxial Fatigue Assessment of Welded Joints—Recommendations for Design Codes, International Journal of Fatigue, Vol. 31, No. 1, 2009, pp. 173–187.
- [15] Bae, D., Sohn, I., and Hong, J., Assessing the Effects of Residual Stresses On the Fatigue Strength of Spot Welds, Welding Journal, Vol. 82, 2003, pp. 18–23.
- [16] Krasovsky, S., Sonnichsen, S., and Bachmann, D., On the Residual Stresses in Multi-Pass Welds: Coupling of Welding Simulation and Fatigue Analysis, Procedia Engineering, Vol. 10, 2011, pp. 506–511.
- [17] Socie, D., Marquis, G., Multiaxial Fatigue: Warrendale, Society of Automotive Engineers Inc, 2000.
- [18] Vasantharaja, P., Maduraimuthu, V., Vasudevan, M., and Palanichamy, P., Assessment of Residual Stresses and Distortion in Stainless Steel Weld Joints, Materials and Manufacturing Processes, Vol. 27, No. 12, 2012, pp. 1376–1381.
- [19] Yuguang, C., Zhanbin, M., Shihua, Z., and Haiqing, T., FEM Study On the Stress Concentration factors of K-Joints with Welding Residual Stress, Applied Ocean Research, Vol. 43, 2013, pp. 195–205.
- [20] Ganesh, K., Vasudevan, M., Balasubramanian, K., Chandrasekhar, N., and Vasantharaja, P., Thermo-Mechanical Analysis of TIG Welding of AISI 316 LN

- Stainless Steel, *Materials and Manufacturing Processes*, Vol. 29, No. 8, 2014, pp. 903–909.
- [21] Vasantharaja, P., Vasudevan, M., and Palanichamy, P., Effect of Welding Processes On the Residual Stress and Distortion in Type 316LN Stainless Steel Weld Joints, *Journal of Manufacturing Processes*, Vol. 19, 2014, pp. 187- 193.
- [22] Bhatti, A. A., Barsoum, Z., Murakawa, H., and Barsoum, I., Influence of Thermo-Mechanical Material Properties of Different Steel Grades On Welding Residual Stresses and Angular Distortion, *Materials and Design*, Vol. 65, 2015, pp. 878–889.
- [23] Lopez-Jauregi, A., Esnaola, J. A., Ulacia, I., Urrutibeascoa, I., and Madariaga, A., Fatigue Analysis of Multipass Welded Joints Considering Residual Stresses, *International Journal of Fatigue*, Vol. 79, 2015, pp. 75- 85.
- [24] Lopez-Jauregi, A., Ulacia, I., Esnaola, J. A., Ugarte, D., and Torca, I., Procedure to Predict Residual Stress Pattern in Spray Transfer Multipass Welding, the *International Journal of Advanced Manufacturing Technology*, Vol. 76, No. 9-12, 2014, pp. 2117-2129.
- [25] Wang, D., Zhang, H., Gong, B., and Deng, C., Residual Stress Effects On Fatigue Behaviour of Welded T-Joint: A Finite Fracture Mechanics Approach, *Materials and Design*, Vol. 91, 2016, pp. 211- 217.
- [26] Forouzan, M. R., Heidari, A., and Golestaneh, S. J., FE Simulation of Submerged arc Welding of API 5L-X70 Straight Seam Oil and Gas Pipes, *Journal of Computational Methods in Engineering (ESTEGHLAL)*, Vol. 28, No. 1, 2009, pp. 93-110.
- [27] Forouzan, M. R., MirfalahNasiri, S. M., Mokhtari, A., Heidari, A., and Golestaneh, S. J., Residual Stress Prediction in Submerged arc Welded Spiral Pipes, *Materials & Design*, Vol. 33, 2012, pp. 384-394.